Catalysis
Science & Technology

RSC Publishing

PAPER

View Article Online
View Journal



Cite this: DOI: 10.1039/c3cy00232b

# Asymmetric benzoylation of hydrobenzoin by copper(II) bis(oxazoline) anchored onto ordered mesoporous silicas and their carbon replicas†

Ana Rosa Silva,*[a] Liliana Carneiro,[a] Ana P. Carvalho[b] and João Pires[b]

Received 10th April 2013,
Accepted 24th June 2013

DOI: 10.1039/c3cy00232b

www.rsc.org/catalysis

A copper(II) complex with a commercial chiral bis(oxazoline) was anchored onto ordered mesoporous silica materials and their respective carbon replicas. The amount of transition metal complex loaded onto the mesostructured solids was determined by ICP-AES and the materials were also characterized by elemental analysis, FTIR, TG/DSC and isotherms of $N_2$ adsorption at −196 °C. For the first time the asymmetric benzoylation of a 1,2-diol was performed in the heterogeneous phase by using an anchored commercial bis(oxazoline) ligand. The effect of the type of mesoporous material on the catalytic parameters, as well as on the reutilization of catalysts in several catalytic cycles, was checked. All the composites prepared were active, selective and enantioselective in this asymmetric organic transformation. Using the two ordered mesoporous silicas as supports good selectivities, with comparable yields and TONs to the homogeneous phase reaction, were obtained. Furthermore these two heterogeneous catalysts are more stable upon reuse than the corresponding ordered carbon replica materials. One of the former heterogeneous catalysts, with mesoporous silica as a support, could be further reused for 4 consecutive cycles without significant loss of selectivity, the TON or enantioselectivity.

## 1. Introduction

Bis(oxazoline) ligands, Box (Scheme 1), are privileged chiral ligands and their copper(II/I) complexes are versatile enantioselective and efficient homogeneous catalysts in a number of asymmetric organic transformations,[1–6] such as the cyclopropanation[2–5,7] and aziridination[8,9] of alkenes and kinetic resolution of 1,2-diols.[10] Heterogeneous catalysts, however, would be preferable due to several inherent practical advantages associated with separation, handling, stability, recovery and re-use.[2–5,11] Furthermore, bis(oxazoline) ligands are synthesized from expensive chiral aminoalcohols with moderate to good yields,[12] making them excellent and desirable candidates for heterogenization using solid supports in order to make them recyclable and economical catalysts. Most of the reports on the heterogenization of copper(II) bis(oxazoline) are on organic polymers.[2–5,11] Ordered mesoporous silicas present, however, higher specific surface area, mechanical resistance, chemical robustness and thermal stability than organic polymers.

On the other hand, porous carbon materials (*e.g.* activated carbons) possess several advantages over the inorganic porous solids, such as the hydrophobic nature of their surfaces, high specific surface area, large pore volumes, chemical inertness and good mechanical stability.[13] Its tunable surface chemistry rich in oxygen functional groups[14] also allows for wider strategies of homogeneous catalyst anchoring than the inorganic solids.[15–21] However activated carbons are mostly microporous, thus their application as a support for large transition metal complexes is restricted. Only in 1999 preparation of the first ordered mesoporous carbon making use of the ordered mesoporous inorganic solids as templates was reported.[22] These solids possess high surface areas and uniform mesopores, although accompanied by a certain amount of micropores.[22,23] More recently, practical and faster ways of preparing mesoporous carbon materials have also been reported.[24,25] The use of ordered mesoporous carbon solids as supports in asymmetric catalysis is still in its infancy, despite the potential advantages compared with the ordered inorganic mesoporous solids. Besides our work with anchored copper(II)

[a] Departamento de Química, CICECO, Universidade de Aveiro, Campus Universitário de Santiago, 3810-193 Aveiro, Portugal. E-mail: ana.rosa.silva@ua.pt; Fax: +351 234 401 470; Tel: +351 234 370 604
[b] CQB, Departamento de Química e Bioquímica, Faculdade de Ciências, Universidade de Lisboa, 1749-016 Lisboa, Portugal

† Electronic supplementary information (ESI) available: Synthesis of the mesoporous materials, FTIR, UV-vis, HRMS, $^1$H and $^{13}$C NMR spectra of functionalized ligand **2**, HPLC chromatograms, thermo analysis curves for carbon based samples and FTIR spectra of the reused heterogeneous catalysts. See DOI: 10.1039/c3cy00232b

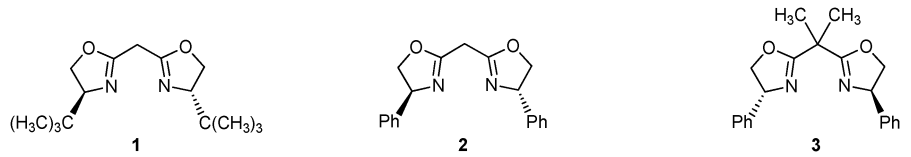


1 2 3

**Scheme 1** Commercial bis(oxazoline) ligands (**1**) *t*ButBox, (**2**) PhBox and (**3**) $Me_2$PhBox.

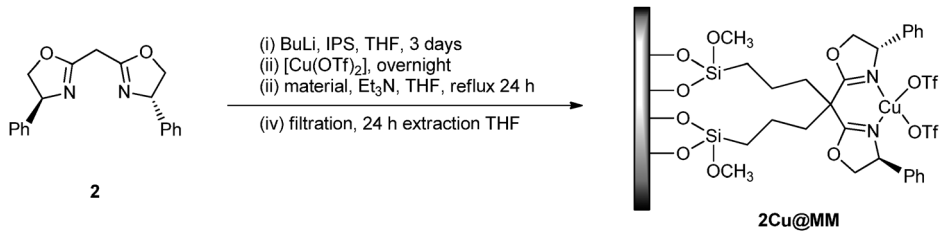


2

**Scheme 2** Anchoring procedure for the **2Cu** complex.



aza-bis(oxazolines) for the asymmetric cyclopropanation of styrene,[26] to the best of our knowledge there are no reports of carbon ordered materials as supports for copper(II) complexes with commercially available, but expensive, bis(oxazoline).

Matsumura *et al.* reported in 2003 that the 5% mol copper(II) chloride complex with bis(oxazoline) ligand **3** (Scheme 1) is a highly enantioselective homogeneous catalyst in the kinetic resolution (or benzoylation) of 1,2-diols at low temperature in dichloromethane.[10] Based on this work Reiser *et al.* reported the efficient asymmetric benzoylation of 1,2-diols by using copper(II) aza-bis(oxazoline) in the homogeneous phase and the immobilized complex,[27] followed by their very efficient and reusable magnetically separable versions.[28,29] However this type of ligand is not commercially available and thus the lack of reports on the mono-benzoylation of 1,2-diphenyl-1,2-ethanediol using immobilized commercial bis(oxazoline) prompted us to test in this reaction the **2Cu** complex anchored onto the surface of various supports, using a reported procedure (Scheme 2).[30] Unexplored ordered mesoporous carbon materials and their mesoporous silica precursors were also used as supports with the aim of checking the effect of their nature (inorganic *vs.* carbon) on the catalytic performance and stability upon reuse. Because we have also been investigating eventual confinement effects within pores of materials,[31,32] the **2Cu** complex was also heterogenized onto smaller pore hexagonal mesoporous silica (HMS).

## 2. Experimental

### 2.1. Materials

Copper(II) trifluoromethanosulfonate (copper triflate, $[Cu(OTf)_2]$ or $[Cu(CF_3SO_3)_2]$, 98%), (*S*)-(−)-2,2′-isopropylidenebis(4-phenyl-2-oxazoline) (**3**, 97%), 2,2′-methylenebis[(4*S*)-4-phenyl-2-oxazoline] (**2**, 97%), butyl lithium solution 1.6 M in hexane, 3-iodopropyltrimethoxysilane (IPS, ≥95.0%), triethylamine ($Et_3N$, ≥99%), dry tetrahydrofuran (THF, ≥99.9%), (*R*,*R*)-1,2-diphenyl-1,2-ethanediol (99%), (*S*,*S*)-1,2-diphenyl-1,2-ethanediol (99%), *N*,*N*-diisopropylethylamine (DIPEA, 99%), benzoyl chloride (99%), potassium hydroxide (p.a.) and potassium bromide (FT-IR grade, ≥99%) were purchased from Aldrich and used as received. Ethanol (p.a.) and methanol (p.a.) were purchased from Riedel de Häen. Dichloromethane, acetonitrile, *n*-hexane, isopropanol and ethyl acetate were purchased from Romil and of HPLC grade. The ESI† includes details of the synthesis of the mesoporous materials and characterization procedures for the hexagonal mesoporous silica (HMS), the SBA-15 material and its carbon replica CMK-3, as well as the silica SPSi and its carbon replica SPC that are prepared in a one step methodology from a silica–carbon composite material.

### 2.2. Preparation and characterization of the homogeneous catalyst (2Cu)

The copper(II) complex with the commercial bis(oxazoline) **2** (Scheme 1) was prepared by dissolution in dichloromethane of equimolar quantities of $[Cu(OTf)_2]$ and **2**, which were stirred for two hours at room temperature. The solution was filtered and upon evaporation of solvent a brown solid precipitated. $CuC_{21}H_{18}F_6N_2O_8S_2$, ESI-MS, *m*/*z*: 674.19 $[M + Li]^+$. FTIR, $\nu$ ($cm^{-1}$): 1612 m, 1259 vs, 1178 s, 1033 s, 642 s.

### 2.3. Anchoring of the 2Cu complex onto the various mesoporous materials

This method has three main steps: (i) functionalization of **2**, (ii) coordination of the copper(II) onto the chiral ligand **2** and (iii) anchoring onto the surface of the material (Scheme 2). Typically, 0.11 mmol of **2** were reacted with 0.29 mmol of butyl lithium (1.6 M in hexane) in 10 ml of dry tetrahydrofuran, under an inert atmosphere. Then the solution was frozen with liquid nitrogen before dropwise addition of 0.36 mmol of 3-iodopropyltrimethoxysilane for 30 minutes.[30] The solution was allowed to warm up and after stirring for 3 days at room temperature, under an inert atmosphere, the colour changed to red-brown, at which point 0.11 mmol of $[Cu(OTf)_2]$ was added and the solution further stirred overnight. Then 0.4 ml of $Et_3N$, 0.50 g of mesoporous material, previously dried at 120 °C for 4 hours, and 5 ml

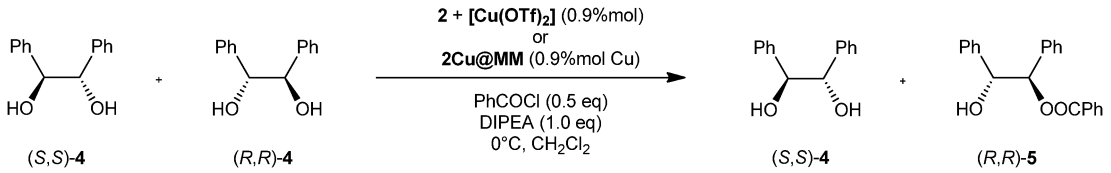


**Scheme 3** Kinetic resolution of 1,2-diphenylethane-1,2-diol.



of dry THF were added to the solution, which was refluxed for 6 hours and stirred over the weekend at room temperature, under an inert atmosphere. The resulting solid was filtered off, washed with 3 × 20 ml of THF, 3 × 20 ml of $CH_2Cl_2$, 3 × 20 ml of methanol and then refluxed with 20 ml of dry THF for 6 hours and stirred overnight at room temperature to remove un-tethered species. Finally, after filtration the solid was dried under vacuum at 60 °C for 2 days.

**2Cu**@SBA-15: elemental analysis (%) N 0.53 C 5.38 H 1.25; ICP-AES Cu 0.64%; loading of **2** 187 μmol $g^{-1}$ and loading of Cu 101 μmol $g^{-1}$.

**2Cu**@CMK-3: elemental analysis (%) N 0.51 C 82.31 H 1.16; ICP-AES Cu 1.11%; loading of **2** 180 μmol $g^{-1}$ and loading of Cu 175 μmol $g^{-1}$.

**2Cu**@SPSi: elemental analysis (%) N 0.59 C 5.90 H 1.15; ICP-AES Cu 0.47%; loading of **2** 209 μmol $g^{-1}$ and loading of Cu 74 μmol $g^{-1}$.

**2Cu**@SPC: elemental analysis (%) N 0.78 C 85.10 H 1.35; ICP-AES Cu 0.66%; loading of **2** 277 μmol $g^{-1}$ and loading of Cu 104 μmol $g^{-1}$.

**2Cu**@HMS: elemental analysis (%) N 0.13 C 2.37 H 1.16; ICP-AES Cu 0.51%; loading of **2** 46 μmol $g^{-1}$ and loading of Cu 80 μmol $g^{-1}$.

### 2.4. Physical and chemical methods

Elemental analysis was performed in duplicate by ''Servicio de Análisis Instrumental'', CACTI Vigo, Universidade de Vigo, Spain. Mass spectroscopy (ESI) was performed at CACTI Vigo, Universidade de Vigo, Spain or at the Mass Spectrometry Centre of the University of Aveiro. The copper ICP-AES was performed at ''Laboratório Central de Análises'' of the University of Aveiro, Portugal. FTIR spectra were collected in the range 400–4000 $cm^{-1}$ at room temperature using a resolution of 4 $cm^{-1}$ and 256 scans and were obtained by attenuated total reflectance (ATR) using a Bruker Tensor 27 spectrophotometer or as KBr pellets with a FT Mattson 7000 galaxy series spectrophotometer (3 mg carbon materials to 200 mg KBr); the samples were dried in an oven at 100 °C for 6 hours prior to the analysis. Thermogravimetry coupled with Differential Scanning Calorimetry (TG-DSC) was performed under air flux, except for the carbon materials where a nitrogen flux was used, with a ramp of 5 °C $min^{-1}$ in a TG-DSC apparatus, model 111 from Setaram. Nitrogen adsorption isotherms at −196 °C were measured in an automatic apparatus (Asap 2010; Micromeritics). Before the adsorption experiments the samples were outgassed under vacuum during 2.5 hours at 150 °C.

### 2.5. Catalysis experiments

All the catalytic reactions of the prepared materials were performed in batch reactors at atmospheric pressure and with constant stirring. The kinetic resolution of 1,2-diphenylethane-1,2-diol was performed at 0 °C using 0.48 mmol (*R*,*R*)-1,2-diphenylethane-1,2-diol, 0.48 mmol (*S*,*S*)-1,2-diphenylethane-1,2-diol, 1.00 mmol DIPEA (170 μl), a heterogeneous catalyst containing 0.9% mol Cu and 0.50 mmol of benzoyl chloride (58 μl) in 5.00 ml of dichloromethane.[10,29] The mixture was stirred for 24 hours and after filtration of the heterogeneous catalyst the solvent was evaporated from the filtrate and the mono-benzoylated product (**5**, Scheme 3) isolated by column chromatography over silica gel using *n*-hexane–ethyl acetate 3 : 1 as eluent. The enantiomeric excess of **5** was determined by HPLC at 254 nm using a Chiralcel OD column (250 mm × 4.6 ID, 5 μm) and *n*-hexane–isopropanol 9 : 1 as eluent. The retention times of the (*R*)-**5** and (*S*)-**5** enantiomers (Scheme 3) were identified by comparison with those of racemic **5** (see Fig. S1 and S2, ESI†). The reaction selectivity (*S*) was calculated based on the isolated yields of **5** and respective enantiomeric excess by using the formulae: $\ln[1 - \text{yield}\,(1 + \text{ee})]/\ln[1 - \text{yield}\,(1 - \text{ee})]$.[10] The isolated materials at the end of the reactions were washed extensively with the appropriate solvent, dried under vacuum and reused in another cycle using the same experimental procedure. Control experiments were also performed using the same experimental procedure in the homogeneous phase with equimolar quantities of $[Cu(OTf)_2]$ plus **2** or **3** in order to compare with the heterogeneous ones.

## 3. Results and discussion

### 3.1. On the alkylation of ligand 2

The functionalization procedure of ligand **2** with 3-iodopropyltrimethoxysilane was adapted from literature and thus it is not new (Scheme 2).[30] Nevertheless, we investigated the UV-visible and FTIR spectra of the original and functionalized ligand **2**. Besides the change in color from light yellow to brown, it is also noteworthy that both UV-visible spectra and FTIR of the functionalized ligand indicate that reaction took place between ligand **2** and 3-iodopropyltrimethoxysilane (IPS). The UV-visible spectrum of the functionalized ligand **2**, shown in Fig. S1 (ESI†), is different from that of ligand **2** and of IPS showing a clear shift of the band from 283 nm to 253 nm accompanied by a decrease in the molar absorptivity of the band, like the one present in the spectrum of the dimethylated ligand **3** (Scheme 1). Moreover, according to the experimental procedure in Section 2.3, the sum of the spectra of ligand **2** plus three

times that of IPS is also different from the one obtained for the functionalized ligand **2**, showing that the reaction took place. From the FTIR spectra, in Fig. S2 (ESI†), a small shift from 1655 to 1651 $cm^{-1}$ in the C=N vibration upon introduction of heavier propyltrimethoxysilane in the central carbon of ligand **2** (Scheme 2) is observed, due to a mass effect. New C–H and Si–O stretching vibrations can also be observed for this functionalized ligand at 2930 and 1028 $cm^{-1}$, respectively.

The propyltrimethoxysilane groups on the functionalized ligand **2** (Scheme 2) prevent further purification of the crude product, as it would graft onto the column silica gel. Therefore, in order to clearly show bi-functionalization of the bis(oxazoline) **2** bridge we were able to isolate both di-methylated (**3**) and di-propylated ligands using the experimental procedure described in Section 2.3. The bis(oxazoline) **3** bearing two methyl groups in the bridge (Scheme 1) was achieved by functionalization of the bis(oxazoline) with iodomethane instead of IPS. The $^1$H NMR spectrum is similar to the commercial bis(oxazoline) **3**, as can be seen in Fig. S3 of ESI.† Whereas the bis(oxazoline) bearing two propyl groups in the bridge was achieved in high yields by functionalization of the bis(oxazoline) with 3-iodopropane instead of IPS (Fig. S4, ESI†). The absence in their $^1$H NMR spectrum of the singlet signal due to the original bridge protons (Scheme 1 and Fig. S3 and S4a of ESI†) and the presence of aliphatic protons clearly show that the di-substitution was successfully achieved. The UV-visible spectrum of the di-propylated bis(oxazoline) **2** (Fig. S1, ESI†) is considerably different from the original ligand **2** and shows a molar absorptivity similar to the one of the dimethylated ligand **3**. The high resolution mass spectrometry (HRMS, ESI) further proved that the di-propylated ligand **2** was synthesized.

It is also noteworthy that the di-propylated bis(oxazoline) **2** was also tested as a homogeneous catalyst in the asymmetric benzoylation of hydrobenzoin. A higher enantioselectivity (94%), and thus selectivity (80), than the original bis(oxazoline) **2** (see Table 2) was obtained showing that the alkylation of the central carbon was achieved.

All together the UV-visible and FTIR data, isolated ligand **3** and di-propylated ligand **2** corroborate the bi-functionalization of ligand **2** with the trimethoxypropylsilane according to Scheme 2.

### 3.2. Materials characterization

Following a reported procedure[30] the 3-iodopropyltrimethoxysilane functionalized copper(II) bis(oxazoline) (**2Cu**) was anchored according to Scheme 2 onto two ordered mesoporous silicas, SBA-15 and SPSi, as well as their carbon replicas, CMK-3 and SPC, respectively. The SPSi and SPC mesoporous materials were prepared by an easier pathway to obtain regular mesoporous materials (silicas and carbons) in one step.[25] With the exception of our previous report,[26] to the best of our knowledge the silicas and carbons obtained by this one step methodology were never studied as supports for inorganic complexes. This complex was also anchored onto a mesoporous silica with much smaller pore size, HMS, to check the effect of the material's pore size on the catalytic parameters. As shown in Scheme 2, the alkoxy groups of the functionalized **2Cu** complex react with the silanol groups on the surface of the mesoporous silicas and the surface phenol groups of the carbon materials, similar to our previous work on the immobilization of homogeneous catalysts onto activated carbons.[18,19] As described in the Experimental section, at the end of the anchoring procedure the materials were extensively washed and refluxed in order to eventually remove the physisorbed catalyst. Thus simple physisorption onto the carbon surface can be ruled out, besides π–π interactions, since the ligand **2** does not present an extended π system, like the previously explored *salen* ligands.[20] This is also supported by the fact that the **2Cu**@SPC and **2Cu**@CMK-3 heterogeneous catalysts do not deactivate upon reuse (see Section 3.3).

**Composition.** In order to determine the amount of ligand **2** immobilized in the materials they were characterized by elemental analysis. The loading of **2** is compiled in Table 1 and it was calculated based on the nitrogen content of the materials since the molecule **2** possesses two nitrogen atoms (Scheme 1). It can be seen that the order of the chiral ligand loading is: SPC > SPSi > SBA-15 ≈ CMK-3 ≫ HMS. Despite their lower superficial area (Table 1, see section Nitrogen adsorption at −196 °C), the mesoporous materials prepared using the one pot procedure (SPC and SPSi) have higher **2** loading than SBA-15 and its carbon replica, CMK-3. Moreover, the SPC mesoporous carbon material has higher **2** loading than the corresponding SPSi mesoporous silica which could be attributed to its higher superficial area (Table 1, see section Nitrogen adsorption at −196 °C). However SBA-15 and CMK-3 possess similar **2** loadings. Among the mesoporous silicas the efficiency of anchoring of the functionalized ligand **2** was 21, 85 and 95% for HMS, SBA-15 and SPSi, respectively.

In order to prevent the creation of nonenantioselective active sites by direct coordination to the mesoporous silica silanols, as we found previously,[32] or to the carbon oxygen groups, copper(II) coordination took place before the anchoring step (ii, Scheme 2). The copper content of the materials was obtained by ICP-AES in order to determine the amount of copper coordinated to the ligand **2**. As can be confirmed in Table 1 the amounts of copper are generally lower than those of **2**.

**Table 1** Chemical and textural characteristics of the materials

| | Concentration (μmol $g^{-1}$) | | | Textural properties | | Density (μmol $m^{-2}$) | |
|---|---|---|---|---|---|---|---|
| Sample | Cu[a] | **2**[b] | **Cu/2** | $A_{BET}$ ($m^2$ $g^{-1}$) | $V_{total}$[c] ($cm^3$ $g^{-1}$) | Cu | **2** |
| SBA-15 | | | | 756 | 0.99 | | |
| CMK-3 | | | | 1396 | 1.26 | | |
| SPSi | | | | 571 | 0.84 | | |
| SPC | | | | 1140 | 1.23 | | |
| HMS | | | | 994 | 0.72 | | |
| **2Cu**@SBA-15 | 101 | 187 | 0.5 | 556 | 0.79 | 0.13 | 0.25 |
| **2Cu**@CMK-3 | 175 | 180 | 1.0 | 529 | 0.65 | 0.13 | 0.13 |
| **2Cu**@SPSi | 74 | 209 | 0.4 | 404 | 0.62 | 0.13 | 0.37 |
| **2Cu**@SPC | 104 | 277 | 0.4 | 719 | 0.75 | 0.09 | 0.24 |
| **2Cu**@HMS | 80 | 46 | 1.7 | 667 | 0.50 | 0.08 | 0.05 |

[a] Determined by ICP-AES. [b] Determined by EA from the nitrogen content. [c] Calculated from the nitrogen adsorption isotherm at $p/p^0 = 0.95$.[36]

This result suggests that the formation constant of complex **2Cu** is not high and that the complexation of copper(II) to the ligand **2** is weak.[33] It is curious to note that the copper contents are not in line with the loadings of **2** and that the CMK-3 material has the highest copper content followed by the other mesoporous carbon, SPC, and the mesoporous silicas, SBA-15 and SPSi, with lower copper contents than the corresponding mesoporous carbons.

**FTIR.** The FTIR spectra of the mesoporous silica materials, SBA-15, SPSi and HMS, are dominated by the Si–O asymmetric and symmetric stretching vibrations, respectively, at 1050 and 800 $cm^{-1}$ (Fig. 1). Moreover by ATR a low intensity peak at 3746 $cm^{-1}$ can be distinguished in the spectra of these materials, which is due to the stretching of the O–H groups from the isolated silanols.[34] Although the samples were dried for 6 hours at 100 °C under vacuum O–H stretching and bending vibrations around 3450 and 1640 $cm^{-1}$, respectively, from adsorbed water can still be observed. The carbon mesoporous materials, CMK-3 and SPC, show very low intensity broad bands also around 3500 and 1639 $cm^{-1}$ which may be due to the O–H stretching and bending vibrations, respectively, of adsorbed water, as well as a broad band at 1100 $cm^{-1}$ probably due to the Si–O stretching vibration of remaining silica templates.

In the materials containing the anchored **2Cu**, besides the characteristic bands of the materials very low intensity bands between 2930–2850 and 1460–1400 and at 700 $cm^{-1}$ due to vibrations characteristic of the ligand **2** can be further seen (Fig. 1f). As can be seen in Fig. 1f these characteristic vibrations are generally low in intensity, which decreases upon copper(II) coordination. Hence it is very difficult to detect clearly the characteristic bands of this last molecule upon anchoring onto the several solid supports. The characteristic strong stretching C=N vibration of the ligand **2** can be seen at 1655 $cm^{-1}$, which shifts to 1520 $cm^{-1}$ upon copper(II) coordination (Fig. 1f) and is generally masked by the large O–H bending vibration of the water adsorbed on the surface of the silica based materials centered at about 1625 $cm^{-1}$. Nonetheless, in the case of the SPC it can be clearly seen at 1614 $cm^{-1}$, according to vibration of the **2Cu** complex (Fig. 1f). Also due to the higher ligand **2**

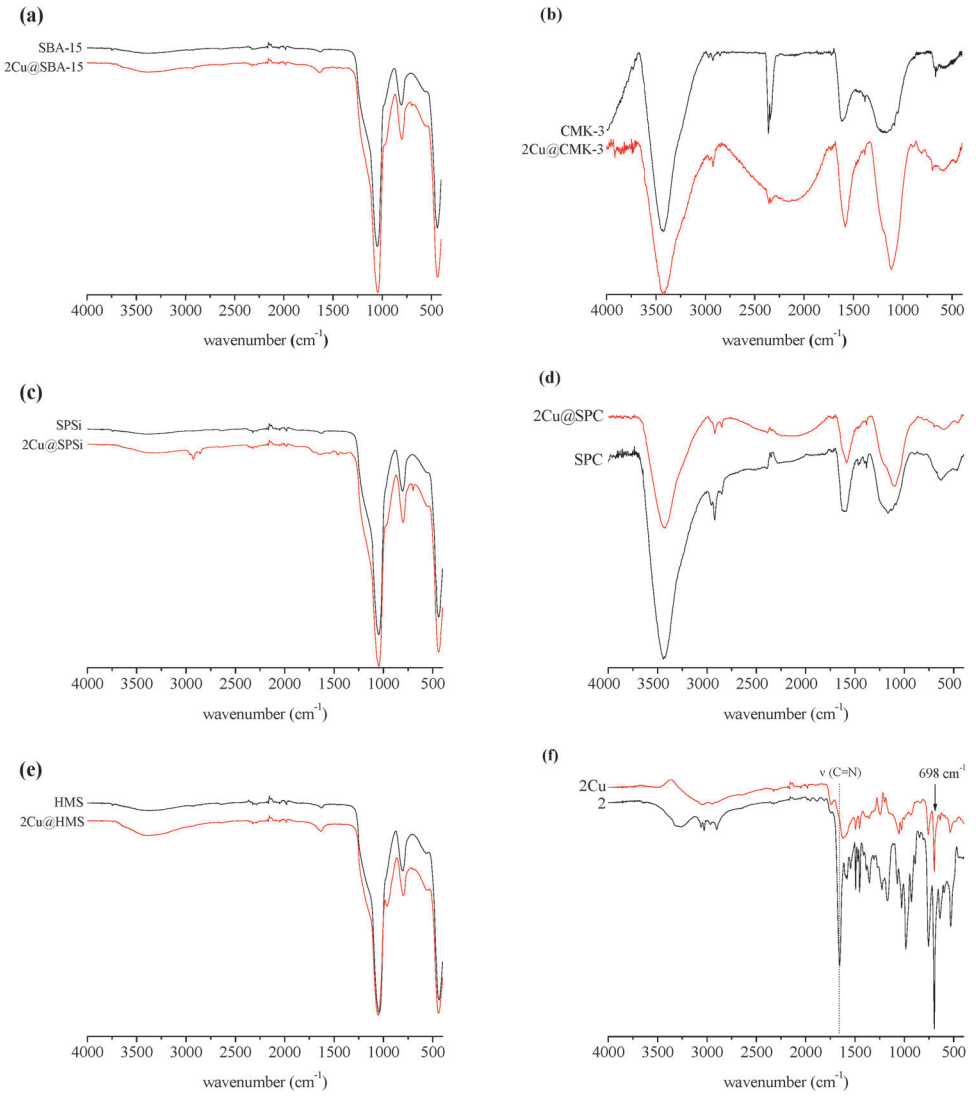


**Fig. 1** FTIR spectra (ATR for silica materials and KBr pellets) for: (a) SBA-15, (b) CMK-3, (c) SPSi, (d) SPC and (e) HMS materials and (f) **2** and **2Cu**.

loading its characteristic vibrations can be clearly observed in the **2Cu**@SPSi material than in the other materials. Furthermore the low intensity band at 3746 $cm^{-1}$, due to the stretching of the O–H groups from the isolated silanols of the mesoporous silicas, disappeared confirming that grafting between these groups and the propylsilane functionalized **2Cu** took place according to Scheme 2.[34]

**TG-DSC.** TG-DSC for the silica based materials was obtained under air flux and is presented in Fig. 2. The results obtained for the carbon based samples are less informative because they were obtained not under air but under nitrogen, otherwise the carbon matrix would be consumed (Fig. S5, ESI†). All silica materials, before functionalization with the **2Cu** complex present an initial mass loss, below 150 °C, with a corresponding endothermic peak in the DSC curve, ascribed to the loss of physisorbed water. The amount of water loss is not necessarily in line with the total porous volume of the samples (Table 1) since water adsorption is also dependent on the nature of the surface chemistry of the material.[35] Examples of this are the SPSi and the HMS samples, for which SPSi has 0.84 $cm^3\ g^{-1}$ of porous volume and loses 3.9% of mass while HMS has 0.72 $cm^3\ g^{-1}$ of porous volume but loses 7.7% of mass. In the case of the samples with the **2Cu** complex, the initial fall in the TG curve is also noticed but the mass loss process is much more continuous with temperature suggesting that the decomposition of functionalized species starts at temperatures around 200 °C. In fact, at this temperature, an exothermic transformation, which can be ascribed to the reaction of organic surface species with the oxygen flow, starts to be noticed in the DSC curve. This transformation as a peak near 325 °C, for **2Cu**@SBA-15 and **2Cu**@HMS, and 365 °C for the **2Cu**@SPSi sample, is ascribed to the complex decomposition. This peak is also much sharper for the **2Cu**@SPSi sample as a most probable consequence of the complex being more homogeneously distributed in this sample.

Considering the results of the nitrogen chemical analysis (Table 1), and the molecular mass of the organic part of the complex, the expected mass loss due to the complex oxidation in air would be 11.3% and 12.6% for SBA-15 and SPSi, respectively. These values are in agreement with the TG data in Fig. 2, if the mass loss for initial materials is subtracted. For the HMS sample, the mass loss obtained by TG is higher than expected on the basis of the chemical analysis. Additionally, for this sample the DSC peak is also much broader that for the other two silicas. Due to the smallest pore sizes of HMS (see below), occlusion of organic molecules from the experimental procedure of the anchoring of the metal complex cannot be entirely ruled out and could justify the broadness of the DSC peak and the excess of mass loss by TG when compared with the nitrogen chemical analysis.

For the carbon replicas CMK-3 and SPC the TG curves also register an initial fall, due to water loss and, for the samples functionalized with the **2Cu** an inflexion in the TG curve is noticed for temperatures between 325–350 °C suggesting that the thermal stability of the supported complex is similar in the silicas and in their carbon replicas (Fig. S4, ESI†).

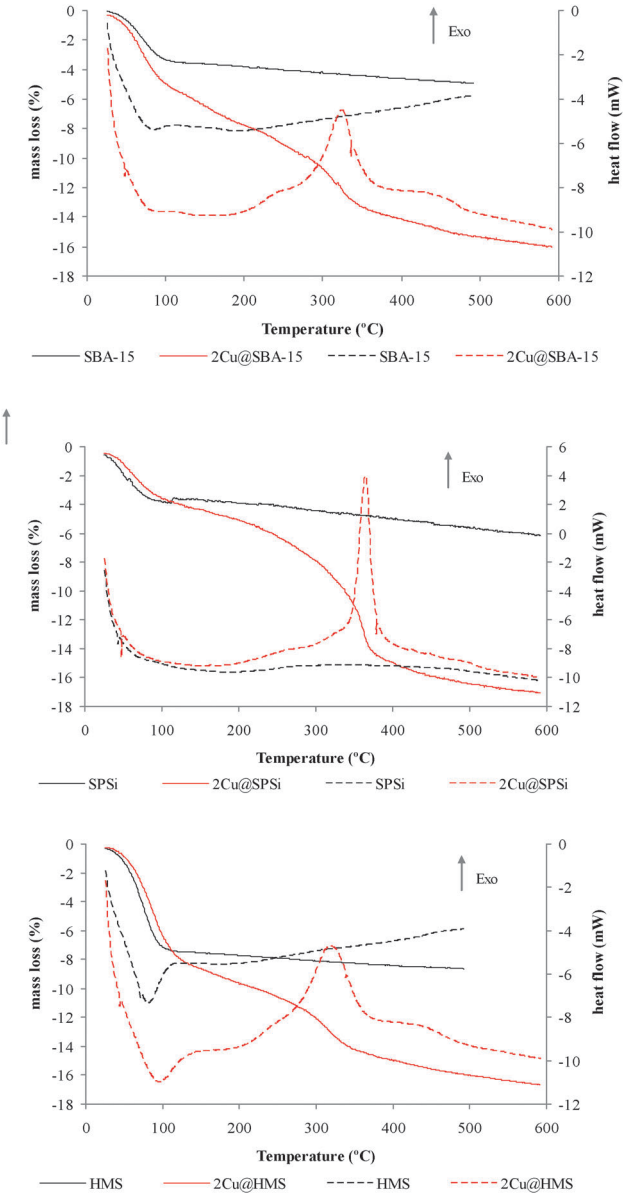


**Fig. 2** Thermo analysis curves for silica based samples. Solid lines for thermogravimetric data (TG) and broken lines for Differential Scanning Calorimetry (DSC) data.

**Nitrogen adsorption at −196 °C.** Nitrogen adsorption–desorption isotherms, at −196 °C, and mesopore size distributions obtained by the Broekhoff–de Boer method[35] are presented in Fig. 3 and 4 for the silicas and their carbon replicas, respectively. In general, the curves are of type IV as expected for mesoporous materials.[36] As noticed in Table 1, and in line with previous results in the literature, the specific surface areas and pore volumes of the carbon replicas are higher than the respective silica templates.[25,37] Conversely, as displayed in Fig. 3b and 4b, the mesoporous size distributions of the silicas are more uniform than those of the respective replicas. Upon the anchoring of the **2Cu** complex, the decrease in the adsorption capacity is clear for all samples, but is more notorious for the carbon replicas (Table 1). Additionally, upon anchoring, the

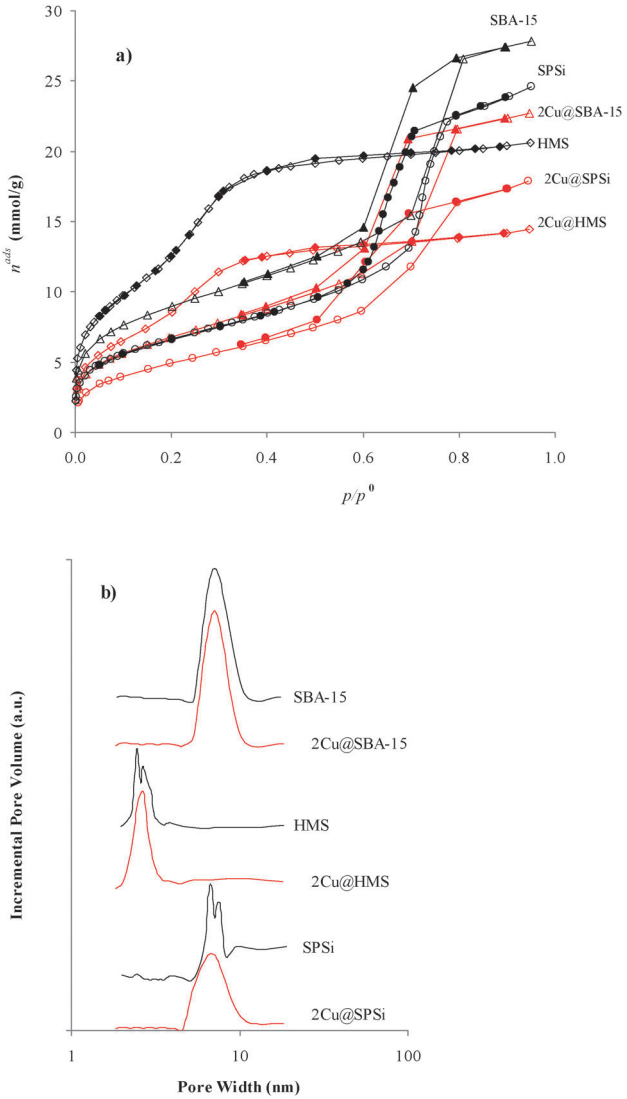


**Fig. 3** (a) Nitrogen adsorption–desorption isotherms, at −196 °C and, (b) mesopore size distributions obtained by the Broekhoff–de Boer method,[21] for the silica based samples.

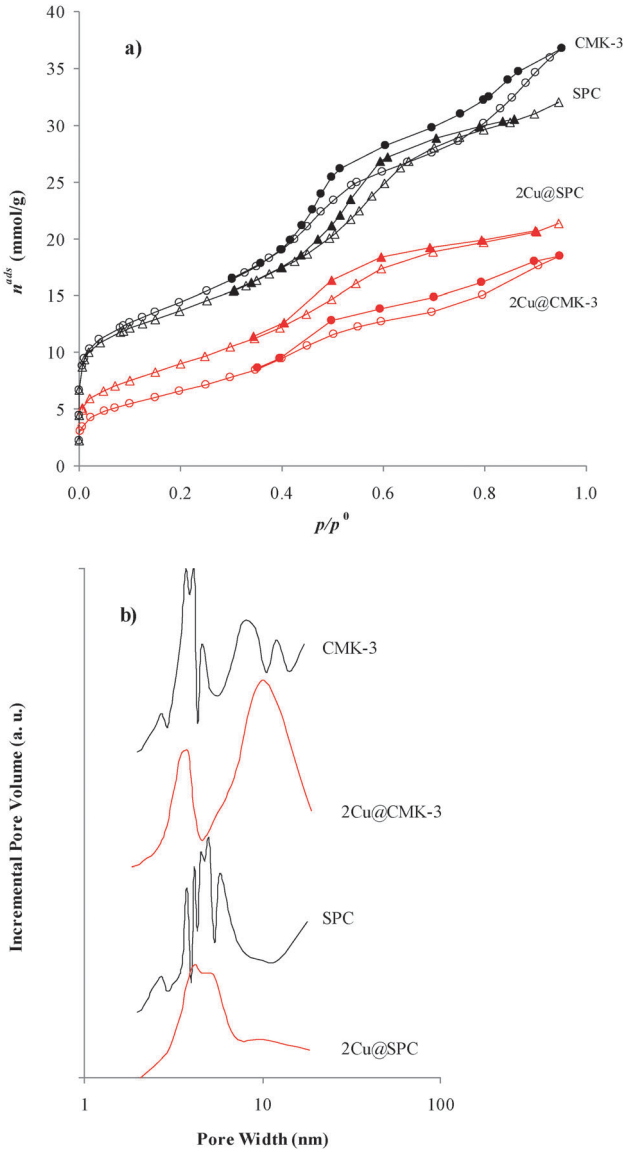


**Fig. 4** (a) Nitrogen adsorption–desorption isotherms, at −196 °C and, (b) mesopore size distributions obtained by the Broekhoff–de Boer method,[21] for the carbon based samples.

mesopore size distributions of both, silica and replicas are not significantly changed except for the CMK-3 material. For this solid (Fig. 4b), the relative intensities of the maxima at near 8.5–10 nm and near 4 nm are reversed after the inclusion of the complex. This suggests that the **2Cu** complex is essentially located in the latter pores, justifying the drastic decrease of the pore volume upon anchoring, as these pores represent the highest proportion of the porosity in CMK-3 as discussed in detail elsewhere.[23]

### 3.3. Catalysis experiments

The copper(II) chloride complex with bis(oxazoline) ligand **3** (Scheme 1) is a highly enantioselective homogeneous catalyst in the mono-benzoylation of 1,2-diols at low temperature in dichloromethane.[10] This prompted us to test the immobilized **2Cu** complex with various supports in this reaction (Scheme 3) under the reported conditions with the aim of checking the effect of properties of the mesoporous support on the catalytic performance of the anchored commercial **2Cu** catalyst. The results are compiled in Table 2 and the characterization of the mono-benzoylated hydrobenzoin is given in ESI† (Fig. S6 and S7).

It can be seen that all the materials prepared act as heterogeneous catalysts in the kinetic resolution of 1,2-diphenyl-1,2-ethanediol at 0 °C in just 0.9% mol based on copper content. High to good selectivities ($S$ = 18–5) with high to moderate enantioselectivities (82–60%) and yields (40–29%) of **5** mono-benzoylated alcohol (Scheme 3) were obtained. The best selectivities were obtained for the mesoporous silicas with 18 (82% ee and 41% yield) for the **2Cu**@SPSi, 16 (81% ee and 40% yield) for the **2Cu**@SBA-15 sample and a much lower 7 (69% ee and 29% yield) for the **2Cu**@HMS sample. The lower catalytic

**Table 2** Kinetic resolution of 1,2-diphenylethane-1,2-diol with **2Cu** anchored onto various porous supports and in the homogeneous phase (Scheme 3)[a]

| | | | mol[b] (%) | | Yield[c] | | | |
|---|---|---|---|---|---|---|---|---|
| | $t$ (h) | Run | Cu | Box | (%) | ee[d] (%) | $S$[e] | TON[f] |
| $CuCl_2{\cdot}2H_2O$ | 2 | | 5.5 | | 38 | 0.1 | 1.0 | 7 |
| (*R*,*R*)-**3**+$CuCl_2{\cdot}2H_2O$ | 2 | | 5.6 | 4.8 | 44 | 95 (*S*,*S*) | 88 | 8 |
| (*S*,*S*)-**2**+$CuCl_2{\cdot}2H_2O$ | 2 | | 5.4 | 4.8 | 42 | 79 (*R*,*R*) | 15 | 8 |
| (*S*,*S*)-**2**+[$Cu(OTf)_2$] | **24** | | **1.0** | **1.0** | **46** | **84** (*R*,*R*) | **27** | **46** |
| (*S*,*S*)-**3**+[$Cu(OTf)_2$] | 24 | | 1.0 | 1.0 | 47 | >99 | >581 | 45 |
| without catalyst | 24 | | | | 21 | 0 | | |
| (*S*,*S*)-**2Cu**@SBA-15 | **24** | **1st** | **0.9** | **1.7** | **40** | **81** (*R*,*R*) | **16** | **42** |
| | 24 | 2nd | 0.9 | 1.6 | 39 | 76 (*R*,*R*) | 12 | 45 |
| (*S*,*S*)-**2Cu**@CMK-3 | **24** | **1st** | **0.9** | **1.0** | **40** | **64** (*R*,*R*) | **6.9** | **42** |
| | 24 | 2nd | 0.8 | 0.8 | 38 | 53 (*R*,*R*) | 3.5 | 49 |
| (*S*,*S*)-**2Cu**@SPSi | **24** | **1st** | **0.9** | **2.7** | **41** | **82** (*R*,*R*) | **18** | **44** |
| | 24 | 2nd | 0.9 | 2.5 | 34 | 79 (*R*,*R*) | 13 | 38 |
| | 24 | 3rd | 0.8 | 2.3 | 35 | 79 (*R*,*R*) | 13 | 43 |
| | 24 | 4th | 0.8 | 2.2 | 36 | 82 (*R*,*R*) | 16 | 46 |
| (*S*,*S*)-**2Cu**@SPC | **24** | **1st** | **0.9** | **2.5** | **35** | **60** (*R*,*R*) | **5.4** | **38** |
| | 24 | 2nd | 0.8 | 2.1 | 38 | 36 (*R*,*R*) | 2.5 | 47 |
| (*S*,*S*)-**2Cu**@HMS | **24** | **1st** | **0.9** | **0.5** | **29** | **69** (*R*,*R*) | **7.2** | **31** |
| | 24 | 2nd | 0.9 | 0.5 | 24 | 59 (*R*,*R*) | 4.6 | 27 |

[a] Reactions performed at 0 °C using 0.48 mmol (*R*,*R*)-**4**, 0.48 mmol (*S*,*S*)-**4**, 1.00 mmol DIPEA, 0.9% mol Cu heterogeneous catalyst and 0.50 mmol of benzoyl chloride in 5.0 ml of $CH_2Cl_2$. [b] % of copper and **2** in the catalyst in relation to **4** (see Table 1); for the recycling experiments corrected for the loss of heterogeneous catalyst weight. [c] Isolated yield of **5** (Scheme 3). [d] Enantiomeric excess of **5** and configuration of the major enantiomer in brackets (Scheme 3), determined by HPLC. [e] Selectivity ($S$) = ln[1 − yield (1 + ee)]/ln[1 − yield (1 − ee)]. [f] TON = moles of isolated **5**/moles of Cu.

performance of **2Cu**@HMS silica might be due to the less efficient distribution of the **2Cu** catalyst on the mesoporous silica matrix which resulted in slightly lower catalyst density (see TG/DSC, Fig. 2, Table 1). The lower mesopore size of the HMS material (2.5 nm) when compared with 7 nm of the SBA-15 and SPSi (Fig. 3), the size of which further decreases upon anchoring of **2Cu** (Fig. 3), may also contribute to its lower catalytic performance. Furthermore, both **2Cu**@SPSi and **2Cu**@SBA-15 present comparable enantioselectivities to the control experiments performed in the homogeneous phase with 1.0% mol of **2** + [$Cu(OTf)_2$] (84%, Table 2) and **2** + $CuCl_2{\cdot}2H_2O$ chloride in 5% mol (79%, Table 2). On the other hand, the selectivities of **5** obtained with the heterogeneous catalysts with the ordered mesoporous carbons are similar to the one with HMS material but lower, with 7 (64% ee and 40% yield) for **2Cu**@CMK-3 and 5 (60% ee and 35% yield) for **2Cu**@SPC. These heterogeneous catalysts present similar copper densities as the heterogeneous catalysts with the parent mesoporous silicas (Table 1) and higher yields than the **2Cu**@HMS catalyst (Table 2). Hence the carbon surface appears not to be appropriate to the course of this asymmetric transformation, ruling out the effect of the smaller mesopore size of both carbon materials (4 nm).

The best heterogeneous catalysts reported herein using the commercial bis(oxazoline) **2** anchored onto the SPSi (82% ee and 41% yield) and SBA-15 (81% ee and 40% yield) mesoporous silica in only 0.9% mol of copper are superior to the kinetic resolution/mono-benzoylation of 1,2-diphenyl-1,2-ethanediol using 5% mol of copper(II) chloride aza-bis(oxazoline) anchored onto the MeOPEG (67% ee and 31% yield)[27,28] and Merrifield resin (82% ee and 36% yield).[28] Reiser *et al.* have also reported more efficient heterogeneous catalysts for the kinetic resolution/mono-benzoylation of 1,2-diphenyl-1,2-ethanediol by using copper(II) chloride complexes with aza-bis(oxazolines) anchored onto supermagnetic magnetite@silicananoparticles (97% ee and 38–46% yield)[28] and magnetic Co/C nanoparticles (97% ee and 47% yield).[29] However the aza-bis(oxazoline)s are not commercially available and have to be synthesized in a 3 step procedure with moderate yield.[38,39] Some sensibility to the acidity of the support surface has also been observed by us in the cyclopropanation of styrene using this type of ligands.[26]

Recycling of the **2Cu**@SPSi heterogeneous catalyst, using the same experimental procedure, gives consistent selectivity and activity at least for four cycles. On the other hand, the other heterogeneous catalysts show consistent activity but decreased selectivity, with a slight decrease in the enantioselectivity and drastic decrease for **2Cu**@SPC (Table 2). Thus no deactivation of the **2Cu**@SPSi heterogeneous catalyst is observed at least for four consecutive reuses under the experimental conditions of the kinetic resolution/mono-benzoylation of 1,2-diphenyl-1,2-ethanediol and a total TON of 171 is reached. This is corroborated by the FTIR spectra of the used materials (see Fig. S8, ESI†).

The best heterogeneous catalysts reported herein also showed superior catalytic behaviour in a second cycle of utilization in the kinetic resolution/mono-benzoylation of 1,2-diphenyl-1,2-ethanediol (Table 2) compared to using 5% mol of copper(II) chloride aza-bis(oxazoline) anchored onto the MeOPEG (62% ee and 43% yield) and Merrifield resin (56% ee and 35% yield):[28] **2Cu**@SPSi (79% ee and 34% yield) and SBA-15 (76% ee and 39% yield). It is also noteworthy that these heterogeneous catalysts were tested in this reaction after more than one year of being prepared. The high activities and enantioselectivities obtained indicate that the commercial ligand **2** is stable upon immobilization with time, irrespective of the mesoporous support surface acidity.[26] Nevertheless, the copper(II) chloride aza-bis(oxazoline) anchored onto the supermagnetic magnetite@silicananoparticles (95–98% ee and 43–49% yield, 5 cycles)[28] and magnetic Co/C nanoparticles (96–99% ee and 43–49% yield, 5 cycles)[29] are superior to the best heterogeneous catalysts reported herein.

## 4. Conclusions

A copper(II) complex with a commercial chiral bis(oxazoline) (**2Cu**) was anchored onto ordered silica mesoporous materials and their carbon replicas with a generally higher amount of chiral ligand than copper. All the composites prepared were active and enantioselective in the kinetic resolution/mono-benzoylation of 1,2-diphenyl-1,2-ethanediol at 0 °C in just 0.9% mol based on copper content with high to good

selectivities (18–13), with high to moderate enantioselectivities (82–60%) and yields (41–29%, with a maximum of 50% corresponding to the kinetic resolution of one enantiomer). Furthermore, comparable enantioselectivity and activity to the homogeneous phase was obtained with **2Cu**@SPSi and **2Cu**@SBA-15. Moreover, the ordered mesoporous silicas, SBA-15 and SPSi, yield more selective heterogeneous catalysts than when the corresponding mesoporous carbon replicas are used as homogeneous catalyst supports. Therefore the more uniform mesopore size distributions of the silica materials may be a more relevant factor than, for instance, the total pore volume, and/or the type of matrix support, *i.e.* carbon *vs.* silica. Among the silica materials, the heterogeneous catalysts with the smaller mesopores (HMS) showed significantly lower selectivity.

The **2Cu**@SPSi heterogeneous catalyst can be recycled with consistent activity and selectivity at least 4 times for the kinetic resolution/mono-benzoylation of 1,2-diphenyl-1,2-ethanediol, with almost quantitative recovery by simple filtration and a total TON of 171. Therefore the ordered mesoporous silicas are better supports for the **2Cu** homogeneous catalyst than the ordered carbon materials for this reaction.

In this work we were able to show that a copper(II) complex with an expensive commercial bis(oxazoline) anchored onto a mesoporous silica (SPSi), prepared using a simple procedure, is a stable heterogeneous catalyst for the kinetic resolution/mono-benzoylation of 1,2-diphenyl-1,2-ethanediol.

## Acknowledgements

This work was funded by Fundação para a Ciência e a Tecnologia (FCT) through the project PTDC/QUI/64770/2006, which was co-financed by EU under the programs COMPETE, QREN and FEDER. ARS thanks FCT, FSE and POPH for the contracts under the programs *Ciência 2008* and *Investigator FCT 2012*, as well as for financing under the program Pest-C/CTM/LA0011/2011 (CICECO) and PEst-OE/QUI/UI0612/2013 (CQB/FC/UL). We would also like to acknowledge Dr Mónica Valega and Prof. Fernando Domingues from the Department of Chemistry of the University of Aveiro for the initial help in the HPLC analytical method development.

## References

1 G. Desimoni, G. Faita and K. A. Jorgensen, *Chem. Rev.*, 2011, **111**, PR284–PR437.
2 J. M. Fraile, J. I. Garcia, C. I. Herrerias, J. A. Mayoral, E. Pires and L. Salvatella, *Catal. Today*, 2009, **140**, 44–50.
3 A. F. Trindade, P. M. P. Gois and C. A. M. Afonso, *Chem. Rev.*, 2009, **109**, 418–514.
4 J. M. Fraile, J. I. Garcia and J. A. Mayoral, *Chem. Rev.*, 2009, **109**, 360–417.
5 J. M. Fraile, J. I. Garcia, C. I. Herrerias, J. A. Mayoral and E. Pires, *Chem. Soc. Rev.*, 2009, **38**, 695–706.
6 M. Bartok, *Chem. Rev.*, 2010, **110**, 1663–1705.
7 D. A. Evans, K. A. Woerpel, M. M. Hinman and M. M. Faul, *J. Am. Chem. Soc.*, 1991, **113**, 726–728.
8 D. A. Evans, M. M. Faul and M. T. Bilodeau, *J. Org. Chem.*, 1991, **56**, 6744–6746.
9 D. A. Evans, M. M. Faul, M. T. Bilodeau, B. A. Anderson and D. M. Barnes, *J. Am. Chem. Soc.*, 1993, **115**, 5328–5329.
10 Y. Matsumura, T. Maki, S. Murakami and O. Onomura, *J. Am. Chem. Soc.*, 2003, **125**, 2052–2053.
11 D. Rechavi and M. Lemaire, *Chem. Rev.*, 2002, **102**, 3467–3493.
12 D. A. Evans, G. S. Peterson, J. S. Johnson, D. M. Barnes, K. R. Campos and K. A. Woerpel, *J. Org. Chem.*, 1998, **63**, 4541–4544.
13 V. Calvino-Casilda, A. J. Lopez-Peinado, C. J. Duran-Valle and R. M. Martin-Aranda, *Catal. Rev. Sci. Eng.*, 2010, **52**, 325–380.
14 J. L. Figueiredo, M. F. R. Pereira, M. M. A. Freitas and J. J. M. Órfão, *Carbon*, 1999, **37**, 1379–1389.
15 A. R. Silva, V. Budarin and J. H. Clark, *ChemCatChem*, 2013, **5**, 895–898.
16 A. R. Silva, C. Freire and B. de Castro, *Carbon*, 2004, **42**, 3027–3030.
17 A. R. Silva, V. Budarin, J. H. Clark, B. de Castro and C. Freire, *Carbon*, 2005, **43**, 2096–2105.
18 A. R. Silva, V. Budarin, J. H. Clark, C. Freire and B. de Castro, *Carbon*, 2007, **45**, 1951–1964.
19 B. Jarrais, A. R. Silva and C. Freire, *Eur. J. Inorg. Chem.*, 2005, 4582–4589.
20 A. R. Silva, M. M. A. Freitas, C. Freire, B. de Castro and J. L. Figueiredo, *Langmuir*, 2002, **18**, 8017–8024.
21 A. R. Silva, J. L. Figueiredo, C. Freire and B. de Castro, *Catal. Today*, 2005, **102**, 154–159.
22 R. Ryoo, S. H. Joo and S. Jun, *J. Phys. Chem. B*, 1999, **103**, 7743–7746.
23 V. K. Saini, M. Andrade, M. L. Pinto, A. P. Carvalho and J. Pires, *Sep. Purif. Technol.*, 2010, **75**, 366–376.
24 C.-C. Ting, H.-Y. Wu, S. Vetrivel, D. Saikia, Y.-C. Pan, G. T. K. Fey and H.-M. Kao, *Microporous Mesoporous Mater.*, 2010, **128**, 1–11.
25 J. Pires, S. Borges, A. P. Carvalho and A. R. Silva, *Adsorpt. Sci. Technol.*, 2010, **28**, 717–726.
26 A. R. Silva, V. Guimarães, A. P. Carvalho and J. Pires, *Catal. Sci. Technol.*, 2013, **3**, 659–672.
27 A. Gissibl, M. G. Finn and O. Reiser, *Org. Lett.*, 2005, **7**, 2325–2328.
28 A. Schatz, M. Hager and O. Reiser, *Adv. Funct. Mater.*, 2009, **19**, 2109–2115.
29 A. Schatz, R. N. Grass, Q. Kainz, W. J. Stark and O. Reiser, *Chem. Mater.*, 2010, **22**, 305–310.
30 R. J. Clarke and I. J. Shannon, *Chem. Commun.*, 2001, 1936–1937.
31 A. R. Silva, H. Albuquerque, A. Fontes, S. Borges, A. Martins, A. P. Carvalho and J. Pires, *Ind. Eng. Chem. Res.*, 2011, **50**, 11495–11501.
32 A. R. Silva, H. Albuquerque, S. Borges, R. Siegel, L. Mafra, A. P. Carvalho and J. Pires, *Microporous Mesoporous Mater.*, 2012, **158**, 26–38.

33 J. M. Fraile, J. I. Garcia, C. I. Herrerias, J. A. Mayoral, O. Reiser, A. Socuellamos and H. Werner, *Chem.–Eur. J.*, 2004, **10**, 2997–3005.
34 A. R. Silva, K. Wilson, A. C. Whitwood, J. H. Clark and C. Freire, *Eur. J. Inorg. Chem.*, 2006, 1275–1283.
35 W. W. Lukens, P. Schmidt-Winkel, D. Y. Zhao, J. L. Feng and G. D. Stucky, *Langmuir*, 1999, **15**, 5403–5409.
36 F. Rouquerol, J. Rouquerol and K. Sing, *Adsorption by Powders and Porous Solids. Principles, Methodology and Applications*, Academic Press, London, UK, 1999.
37 H. F. Yang and D. Y. Zhao, *J. Mater. Chem.*, 2005, **15**, 1217–1231.
38 M. Glos and O. Reiser, *Org. Lett.*, 2000, **2**, 2045–2048.
39 H. Werner, R. Vicha, A. Gissibl and O. Reiser, *J. Org. Chem.*, 2003, **68**, 10166–10168.



 